LATEST RESULTS ON HIGH-P_T JETS IN UA2

The UA2 Collaboration

Presented by
A. R. Weidberg
CERN

ABSTRACT

Results on high p_T jets from the UA2 experiment at the CERN $\bar{p}p$ Collider are presented. The inclusive jet cross sections are found to be in good agreement with QCD predictions, which places limits on the compositeness scale of quarks. The ratio of three jet to two jet events is shown to be a sensitive test of QCD. A status report on the search for exotic events with large missing transverse energy is presented. There was no evidence for any significant signal above background for either monojets or multi-jets with large missing transverse momentum. The data sample corresponds to the 1984 $\bar{p}p$ Collider run ($\sqrt{s}$=630 GeV, $\int \mathcal{L}\, dt$ = 310 nb^{-1}) and all the results presented here are preliminary.

1. INTRODUCTION

The recent unambiguous identification of jets in hadronic collisions[1-4] at the CERN $\bar{p}p$ Collider and at the ISR have allowed for a detailed study of jet production properties and comparisons with QCD predictions. These comparisons showed good agreement between the data and the QCD predictions although the large experimental and theoretical uncertainties imply the need for further more quantitative tests of QCD.

In Section 2 the data taking is briefly reviewed. In Section 3 results are shown on the energy dependence of the inclusive jet cross sections using the 1983 data ($\sqrt{s}$ = 546 Gev) and the 1984 data ($\sqrt{s}$ = 630 Gev). Using a composite model for quarks, limits are placed on possible quark substructure. Results for a search for structure in the two-jet mass spectrum are given in Section 4. In Section 5 results are shown on multi-jet events which provide further tests of QCD. In Section 6 a status report is given on the search for exotic events with large missing transverse energy.

2. DATA TAKING AND REDUCTION

The UA2 detector has been described in detail elsewhere[5]. For the 1984 run four jet triggers were used:

1. two-jet trigger: the total transverse energies in any four consecutive azimuthal modules ($\Delta\phi=15^{0}$) and eight azimuthal modules opposite in ϕ had to exceed both a given threshold (typically 18 GeV),

2. single-jet trigger: the total transverse energy deposited in any eight consecutive azimuthal modules had to exceed a given threshold (typically 30 GeV),

3. total transverse energy trigger: the total tranverse energy collected in the central calorimeter was required to exceed a

threshold, normally set at about 60 GeV except for special low threshold data runs.

4. missing transverse energy trigger: the magnitude of the vector sum of the transverse energy deposited in each of the modules the central calorimeter had to exceed a given threshold (typically 30 GeV).

Background from sources other than $\bar{p}p$ collisions was suppressed at the trigger level by requiring a coincidence of the trigger conditions previously described with two signals (" minimum bias " trigger) obtained from scintillator arrays covering an angular range $0.44^0 \leq \theta \leq 2.84^0$ on both sides of the collision region[6]. The total integrated luminosity accumulated is $\int \mathcal{L}\, dt = 310\ nb^{-1}$. An uncertainty of ± 15 % was estimated for $\int \mathcal{L}\, dt$ from the observed fluctuations during different running conditions and from the overall uncertainty in the cross-section accepted by the " minimum-bias " trigger. The data reduction has been described in detail elsewhere[1].

3. INCLUSIVE JET PRODUCTION CROSS-SECTIONS

The inclusive production cross-sections at $\sqrt{s}$ = 630 GeV are expected to be systematically higher than those at $\sqrt{s}$ = 546 GeV. In order to test this prediction the ratios between the values of the inclusive jet cross sections at $\sqrt{s}$ = 630 GeV and at $\sqrt{s}$ = 546 GeV have been evaluated. The results are presented in figs. 1a and 1b: only the statistical errors have been taken into account, since the systematic contributions are expected to cancel to first order. A p_T (m_{jj}) dependent increase of the jet cross sections is observed as expected from QCD.

The data from UA2 can be compared with those from the ISR[7] in terms of scaled invariant jet cross sections. The "naive" parton model[8] predicts that, as a function of $x_T = 2\, p_T/\sqrt{s}$, the invariant jet cross-section is given by $E\, d\sigma/dp^3 = f(x_T)\, p^{-4}_T$. Fig. 2 shows the quantity $p^4_T\, E\, d\sigma/dp^3$ as a function of x_T both for ISR and UA2 data. As

expected from scale invariance violation, the UA2 data show that at the same x_T the cross sections are lower for higher $\sqrt{s}$.
A phenomenological fit of the form $E\,d\sigma/dp^3 = f(x_T)\,p_T^n$ where $f(x_T) = A\,(1-x_T)^m/x^2{}_T$ was performed. A good overall fit is obtained for all data (ISR at $\sqrt{s}$ = 45 GeV and $\sqrt{s}$ = 63 GeV and UA2 data at $\sqrt{s}$ = 546 GeV and $\sqrt{s}$ = 630 GeV) with the parameters $n = 4.72^{+003}_{-0\cdot06}$, $m = 6.54 \pm 0.15$ and $A = (8.3 \pm 0.4)\ 10^{-27}$. The collider data alone are best described in this context by $n = 4.5 \pm 0.3$, $m = 7.3 \pm 0.2$ and $A = (3.6 \pm 0.2)\ 10^{-28}$.

The good agreement betwen the inclusive cross section data and the QCD predictions allows one to place limits on the possible scale at which quarks are composite. In the context of a particular composite model for quarks and leptons, the effect of compositeness would manifest itself as a new contact interaction visible at large momentum transfer[9]. The inclusive jet cross-sections are expected to deviate at large p_T or m_{jj} from the QCD behaviour depending on the energy scale Λ_c which characterizes the strength of this new interaction. A determination of Λ_c from the data is in principle possible but the uncertainties related to the QCD calculations and the systematic contributions due to the data limit its accuracy. Comparisons between the data and QCD predictions[10] (Λ_c=infinity) show good agreement within the expected systematic errors (see Fig. 3). This can be used to rule out values of Λ_c < 370 GeV at 95% C.L. as seen in Fig. 3.

4. SEARCH FOR STRUCTURE IN THE INVARIANT TWO-JET MASS DISTRIBUTION

Following the indication of a possible structure in the jet-jet invariant mass around 150 GeV as seen in the 1983 data, we repeated the same analysis with higher statistics, for the 1984 data. A sample of clean events with two jets in the central calorimeter and not too much energy in the forward-backward calorimeter were selected. For each event, the two-jet invariant mass was computed increasing the energy of the second jet in order to balance the transverse energy of the first jet ($P_T^{jj} = 0$). The m_{jj} distribution for 1983 and 1984 runs are shown

in figs. 4(a) and (b) respectively. The best description of the data in terms of a smooth distribution is obtained with the following parametrization: $dN/dm_{jj} = \alpha\, e^{\beta m_{jj}} + \gamma\, e^{\delta m_{jj}}$. A simultaneous fit to the data allowing also for the presence of a mass peak was performed. The peak was parametrized by a gaussian with a width of 13 GeV, as expected for the mass resolution in this region. The fit for the 1983 data resulted in an enhancement of $n = 73^{+17}_{-23}$ events at a mass $m = 147 \pm 3$ GeV using only events with $m_{jj} > 80$ GeV. The 1984 data show, on the contrary, no significant structure around $m_{jj} = 150$ GeV. In fact, a fit for a fixed $m_{jj} = 147$ GeV gives a small dip of $n = -47^{+36}_{-50}$ events. Also the combined distribution from the 1983 and 1984 runs has no significant bump above a smooth background: around $m = 147$ GeV, only a "signal" of $n = 26 \pm 42$ events survives.

5. MULTI-JET ANALYSIS

Two-jet production is the dominant hadronic process at large transverse energies at the CERN $\bar{p}p$ Collider[1]. However the fine granularity of the UA2 calorimeter allows for the observation of a clear signal of events with three or more jets. In QCD the main multi-jet event source is the strong radiative correction to the elastic parton-parton scattering processes. The relative rate of three-jet to two-jet events is proportional to the strong interaction coupling constant α_s. A comparison between the two and multi-jet cross-sections gives therefore a determination of α_s. Such an analysis is in progress. We report here only an account of the experimental method together with some preliminary distributions.

Multi-jet events have been studied in a kinematical region where the jets are well separated. This is also the region in which the perturbative QCD calculations[11] give reliable predictions. The "multi-jettiness" of an event is studied in terms of the variables p_{Tout} and the acoplanarity angle ϕ. These two variables measure in fact the lack of planarity of a multi-jet configuration when the collision plane is defined by the proton line of flight (b) and the highest E_T cluster (p_1):

$$\vec{p}_{Tout} = \tfrac{1}{2} \sum_j \left| \frac{\bar{p}_j \cdot (\bar{p}_1 \times \bar{b})}{|\bar{p}_1 \times \bar{b}|} \right|$$

$$\phi_{ij} = -\arccos \left[\frac{(\bar{b} \times \bar{p}_i) \cdot (\bar{b} \times \bar{p}_j)}{|\bar{b} \times \bar{p}_i| \cdot |\bar{b} \times \bar{p}_j|} \right]$$

Fig. 5 displays the distribution of ϕ for three-jet events in an angular region where the two-jet contribution is negligible. A QCD computation[11] for three-parton final states (full line) and a calculation assuming a pure three-parton phase space (dotted line) are also presented in the same figure. The phase space prediction is certainly ruled out and this is a good indication of the sensitivity of this variable to QCD effects.

Fig. 6 shows the distribution of p_{Tout} separately for two and multi-jet events, in the laboratory frame. The results of the predictions of ref 11. for three parton final states obtained with Λ = 200 MeV and normalized to the two-jet sample is also displayed in Fig. 6. All the experimental systematics (luminosity, structure functions, fragmentation, energy scale) are found to be smaller than the theoretical uncertainty. Calculations with different values of Λ result in distributions having the same shape but different absolute normalizations.

6. MISSING TRANSVERSE ENERGY

A search was made for exotic events with large missing transverse energy. The search for events with monojets plus large $\not{p}_T$ was motivated by the UA1 monojet and monophoton events reported in 1983[12]. Multi-jet events with large $\not{p}_T$ are expected to provide a signature for SUSY particle production.

In UA2 there exist two major background sources for the type of events looked for in the present analysis:

a) $\geq$ 2-jet events from genuine $\bar{p}p$ interactions, where $\geq$ 1 jet is at least partially lost in an insensitive region of the detector (see sect. 2). This background is referred to as "QCD background" in the following.

b) Background from beam halo particles, which either satisfy the triggering condition directly or appear as an accidental overlap with a "minimum bias" $\bar{p}p$ interaction. This background is referred to as "beam halo background" in the following.

QCD background events can be recognised if they leave at least some trace of energy in the forward calorimeters opposite in azimuth to the jet (system) seen in the central calorimeter (CC). Thus the forward regions in spite of their lacking hadronic calorimetry can be used as a veto region against the QCD background.

Most of the beam halo background events are easily identified when they satisfy one of the following conditions:

i) if they are associated with an early signal in the small angle scintillator arrays (minimum bias counters),

ii) if the event has an abnormally large total energy fraction in the hadronic compartments,

iii) if the leading central calorimeter cluster has more than 90% of its energy in the hadronic compartments.

Events satisfying any one of the above conditions are rejected. The loss of good events introduced by these cuts has been shown to be negligible [1]. However, while these background rejection criteria are well-suited to the study of two-jet events, they become insufficient when the data of interest are required to have a large missing transverse momentum.

Two scintillator arrays (referred to as veto counters in the following)[+] located at a distance of 8.5 m from the center of UA2 on both sides of the detector and covering a polar angular region of $2.4° < \theta < 7.0°$, are used to reject background events due to beam halo as described below. To further reduce the remaining beam halo background we use the fact that a large fraction of these events is

---

[+] borrowed from the UA5 experiment [13]

characterised by an early timing in either the left or the right hand side veto counter array, depending on the direction of flight of the halo particles (Fig. 7). The sample of early timing events can therefore be used

1. to study the energy deposition pattern of the beam halo background in order to establish suitable cuts other than the timing cut itself (to reduce residual beam halo background due to the inefficiency of the veto counters)

2. to measure the efficiency of these cuts for beam halo background rejection.

The inefficiency on good events of these cuts was measured using balanced two jet events as well as minimum bias events.

7. SEARCH FOR MONOJETS

The search for monojets with the UA2 detector was motivated by the UA1 monojet and monophoton events reported in 1983 [12].

7.1 Monojet Event Selection

The data sample used for the monojet search was the one recorded by the $\not{p}_T$ trigger. For all these events the value of the $\not{p}_T$ was re-determined by software (using the single cell energies), and a $\not{p}_T$ cut was applied at 30 GeV, where the hardware $\not{p}_T$ trigger had been fully efficient. The remaining data sample was subject to the standard UA2 initial selection criteria described in sect. 6 to reject background from non $\bar{p}p$ collisions.

The remaining data sample of 10249 events contains mainly events from the two background sources described in sect. 6, namely QCD events with at least one jet in an insensitive region of the detector, and beam halo background (estimated to account for ≈ 40 % of the present events with $\not{p}_T > 30$ GeV).

At this stage all events are fully reconstructed, and the forward jet energies are recalculated using also the momentum information of the charged tracks.

In the following we describe the specific cuts applied to further reduce the QCD and beam halo background:

a) Keep only events with a sufficiently centred vertex: $|z_{vertex}| < 300$ mm. (The probability to lose jets is higher for largely displaced vertices.)

b) At large distances from the beam the halo induces showers in the outer calorimeter compartments, resulting in leading clusters having a large fraction f_H of their energy in the hadronic compartments. Therefore we require the leading jet (jet1) to have $f_H < 90$ %.

c) In addition we require the leading jet to be well contained in CC by selecting only events where less than half of the energy of jet1 is found in edge cells: $E_{edge\ cells}/E_{tot} < 50$ %.

d) At medium distances the beam halo induces long showers developing in the central calorimeter parallel to the beam line, resulting in characteristic energy patterns. The calorimeter cell array consists of 240 cells arranged in 10 "rings" of cells having a same θ or 24 "slices" of cells having a same ϕ. The largest number N_R of "rings" hit within a wedge of two adjacent "slices" ($N_R \leq 10$) has large values for this configuration. We require $N_R < 7$.

These cuts leave a sample of 3128 events. About 5 % of them are due to beam halo background, which can be further reduced by requiring good timing:

e) We reject events with an early timing in the veto counters by requiring $t_{event} > -23$ ns.

At this stage the beam halo background accounts for only about 1-2 %, and the bulk of the events are of the QCD type: 1 jet in CC, ≥ 1 jet in an insensitive region of UA2. As mentioned in sect. 3 the lost jets usually leave some traces of energy in the forward calorimeters (FC). We therefore impose a cut on the scalar sum of the energies (ΣE_T^{opp}) measured in an azimuthal wedge with half opening angle $\Delta\Phi = 60^\circ$ opposite to the (transverse) direction of the leading jet (QCD events contain mainly 2 jets [1] back-to-back in the transverse plane):

f) ΣE_T^{opp}(in FC alone) < 3 GeV
ΣE_T^{opp}(in FC + CC) < 10 GeV.

The $\not{p}_T$ spectrum of the remaining events is shown in Fig. 8 together with a Monte Carlo prediction for QCD 2-jet background (smooth line) obtained with the ISAJET [14] programme. There is good agreement between our data and the QCD expectation, but a small non QCD type signal can of course not be ruled out.

Above $\not{p}_T = 65$ GeV only one event is present: It has a $\not{p}_T$ of 100.2 GeV, and no track pointing to the energy cluster. Since it has energy in the two inner (i.e. in the electromagnetic and first hadronic) compartments of CC, but none in the outermost (second hadronic), it can neither be interpreted in terms of isolated photons/π^0's nor of ordinary jets. We assume that the event is a beam halo background surviving our cuts. Keeping it, however, in our sample we quote an upper limit on the cross section

$$\sigma = n/\varepsilon \int \mathcal{L} dt \qquad (1)$$

for monojet production in the region $\not{p}_T > 65$ GeV:

$$n(\not{p}_T > 65 \text{ GeV}) < 3.9 \qquad (90\ \%\ \text{c.l.}) \qquad (2)$$

The total cut efficiency ε of the monojet selection has been estimated using minimum bias and balanced two jet events:

$$\varepsilon(\text{monojet cuts}) = 0.54 \qquad (3)$$

This gives for the integrated luminosity of 310 nb^{-1} of the 1984 run:

$$\sigma^{\text{monojet}}(\not{p}_T > 65 \text{ GeV}) < 23 \text{ pb} \quad (90\% \text{ c.l.}) \qquad (4)$$

We can evaluate this upper limit in a somewhat lower $\not{p}_T$-region: There are 40 (218) events with p_t in excess of 50 (40) GeV. Using the region $40 < \not{p}_T < 50$ GeV to normalise the Monte-Carlo calculation, the estimated background from two-jet events in which one of the jets escapes the UA2 acceptance is 46 events for $\not{p}_T > 50$ GeV. From this result the 90% c.l. upper limit for the production of events with a jet plus $\not{p}_T > 50$ GeV is

$$\sigma(\not{p}_T > 50 \text{ GeV}) < 73 \text{ pb (90\% c.l.)} \qquad (4').$$

7.2 Search For Monophotons

As a simple extension of the monojet analysis, a search for monophotons has been carried out, using the final monojet sample of sect. 6.1. and looking for events with isolated electromagnetic clusters. Removing first all known $W \to e\nu$ events the following photon selection cuts were applied (for definitions see ref. [15]):

g) Require the energy cluster to show small lateral extension: cluster radius < 0.5 cells and small leakage into the hadronic compartment.

h) ask for no charged particle track coming from the vertex within a 20° cone around the line from the vertex to the CC energy cluster center. Accept only events with at most one preshower clusters with charge > 3 mip (minimum ionising particle equivalent) in the same 20° cone.

The sample of events with no preshower cluster present is called the "unconverted sample", events with one preshower cluster belong to the "converted" sample.

Fig. 9 shows the p_T-spectrum of the remaining converted and unconverted monophoton candidates. A scanning by physicists on a computerized graphics display (MEGATEK) has shown that out of the five converted events four are probably $W \to e\nu$ events where the electron track has not been reconstructed due to tracking inefficiency.
The conversion probability in the preshower detector is about 70 %. It seems therefore very unlikely, that the unconverted events are due to isolated photons/π^0's. Their much more probable interpretation is in terms of beam halo background.
Estimating the overall efficiency ε of the monophoton search to be

$$\varepsilon(\text{monophoton cuts}) = 0.52 \quad (5).$$

and restricting ourselves to the region p_T^γ >45 GeV, where we observe no event,

$$n(p_T^\gamma > 45 \text{ GeV}, \not{p}_T > 30 \text{ GeV}) < 2.3 \quad (90\ \%\ \text{c.l.}) \quad (6).$$

we quote the following upper limit for the monophoton cross section:

$$\sigma^{\text{monophoton}}(p_T^\gamma > 45 \text{ GeV}, \not{p}_T > 30 \text{ GeV}) < 14 \text{ pb} \quad (90\ \%\ \text{c.l.}) \quad (7).$$

7.3 Search For $W \to e\nu$ Through The $\not{p}_T$ Analysis

Using the process $\bar{p}p \to W+X$, $W \to e\nu$, a cross check can be established between the electron and the $\not{p}_T$ analysis of UA2. To this end events containing electromagnetic clusters and large missing p_T have been selected by extending the present monojet analysis: again, the final monojet candidate sample of sect. 6.1. has been taken and further cuts have been imposed to select electromagnetic clusters:

i) cluster radius < 0.5 cells (as in monophoton search)

ii) hadronic leakage < 12 % (efficiency for 40 GeV electrons: 92 %).

Fig. 9 shows the $\not{p}_T$ spectrum of the remaining events: there is a distinct Jacobian peak at about 40 GeV, indicating as event source the $W \to e\nu$ decay. The smooth curve represents the estimate for background from 2-jets.

This event sample can be compared to that found through the electron search: from the 66 events with $\not{p}_T > 30$ GeV and $p_T^{em} > 30$ GeV, 48 events have been also found in the electron search, the number of non overlapping events thus being 18.
The background estimate for the $W \to e\nu$ search through the $\not{p}_T$ analysis gives an expectation of 7.7 ± 1.0 events from QCD (two-jet) background and 1.1 ± 0.6 events from beam halo background.
In comparison a scan of the non-overlapping events on the MEGATEK graphics display shows that about 9 events can be ascribed to the QCD (two-jet) and about 4 events to the beam halo background, which is roughly compatible with the above estimates. Two events are probably $W \to e\nu$ candidates while the remaining events could not be definitely ascribed to one of the three catagories.

Taking on the other hand the event sample found in the electron search and applying to it the same "filter" cuts as in the monojet analysis,

$E_{edge} < 50$ %; $E_{had}/E_{tot} < 10$ %;

$p_T^e > 30$ GeV; $\not{p}_T > 30$ GeV,

leaves 50 $W \to e\nu$ events in CC, which are reduced to 42 by applying the specific monojet cuts of sect. 7.1 and 7.3. This is in agreement with the efficiency of these cuts as estimated from minimum bias and balanced two-jet events.

A comparison of the two values for the cross section for the process ($\bar{p}p \to W+X$, $W \to e\nu$) shows agreement within errors:

$\sigma(\bar{p}p \to W+X, W \to e\nu) = 590 \pm 90$ pb from $\not{p}_T$ analysis (8a)

$\sigma(\bar{p}p \to W+X, W \to e\nu) = 540 \pm 70$ pb from electron analysis (8b)

8. SEARCH FOR MULTIJET EVENTS WITH $\not{p}_T$

Multi-jet events with $\not{p}_T$ are expected to provide a signature for SUSY particle production at the $\bar{p}p$ Collider. Recent calculations [16-17] indicate that with the present integrated luminosity it is already possible to observe the production of gluinos ($\tilde{g}$) or squarks ($\tilde{q}$) with masses around 50 GeV if they would exist. The dominant sources of g or q production in these models are $\bar{p}p \rightarrow \tilde{g}\tilde{g} + X$, $\tilde{g}\tilde{q} + X$ or $\tilde{q}\tilde{q} + X$ depending on the masses. Each of the g or q decays into ordinary quarks (or gluons) plus a photino ($\tilde{\gamma}$) [16] The final state event topology consists therefore in general of two (or more) unbalanced hadronic jets and $\not{p}_T$ due to the undetected $\tilde{\gamma}$'s.

The main physics background is expected to come from standard QCD production of $\geq$ 3jet events. They can fake such event configurations if one of the jets is badly measured or escapes detection.

8.1 Event Selection

The initial data sample for this analysis (72454 events) consists of events which have at least two jets with $E_T > 15$ GeV inside the fiducial region of the central calorimeter ($|\eta| < 0.85$). The jets are ordered according to decreasing E_T ($E_T^1 > E_T^2 > E_T^3$), and the leading jet is required to fulfill the single jet trigger threshold: $E_T^1 > 30$ GeV.

Multi-jet events with large $\not{p}_T$ have been selected by the criteria $\not{p}_T > 35$ GeV and $15° < \Phi_{12} < 120°$ where Φ_{12} is the azimuthal separation between the two largest jets. Ordinary QCD two-jet events have Φ_{12} strongly peaked towards 180° [1], whereas events with $\Phi_{12} < 15°$ are contaminated by background from beam halo particles. A total of 174 events satisfy this selection. They are submitted to the following cuts which aim at rejecting event configurations where the large $\not{p}_T$ is due to the QCD background from multi-jet events with badly measured jets:

i) $\Sigma E_T(CC) < 20$ GeV, where ΣE_T is the transverse energy summed over all cells of the CC not belonging to the jets;

ii) $\Sigma E_{em}(FC) < 12$ GeV, where ΣE_{em} is the energy summed over all electromagnetic cells of the FC;

iii) $\Phi(p_{T\,J}, \not{p}_{T\,FC}) > 30^\circ$, where $p_{T\,J}$ is the p_T-vector of the jet system and $\not{p}_{T\,FC}$ is the $\not{p}_T$-vector of all cells in the FC alone.

The last two cuts are illustrated in figs. 11 and 12. The distributions of the present event sample are compared with the ones from well-balanced two-jet events (defined by $p_{TJ} < 5$ GeV, $\Phi_{12} > 170^\circ$ and $\not{p}_T < 10$ GeV). In general a significant amount of energy is found in the FC opposite to p_{TJ} in spite of the large overall $\not{p}_T$. This is a clear indication for QCD multi-jet background as mentioned already in sect. 6. The additional FC energy in SUSY events with genuine $\not{p}_T$ is expected to be small and not correlated to p_{TJ} (as for the well-balanced two-jet sample).

Residual beam halo background is rejected by requiring that no veto counter signal be present outside the correct beam-beam interaction window.

8.2 Results

Two events survive the selection criteria. One contains an identified electron, appearing here as the leading jet (E_T^1). The event is of the topology $\bar{p}p \to W+jet+X$, $W \to e\nu$ and is included in the data sample discussed in [18]. There remains only one multi-jet event with $\not{p}_T$. It can most naturally be interpreted in terms of a QCD multi-jet background event because it has $\Phi(p_{T\,J}, p_{T\,FC}) = 42^\circ$ (which is near the cut) and it has also a central calorimeter cluster of $E_T = 7$ GeV opposite to $p_{T\,J}$.

Nevertheless this event is retained in the evaluation of the upper limit on the cross section for multi-jet events with $\not{p}_T > 35$ GeV and $15° < \Phi^{12} < 120°$ The efficiency of the cuts i) to iii) and of the veto counter requirement has been determined experimentally using the sample of well-balanced two-jet events mentioned above. The resulting limit is

$$\sigma^{\text{multijets}+\not{p}_T}(\not{p}_T > 35 \text{ GeV}) < 27 \text{ pb} \quad (90\% \text{ c.l.}) \qquad (9).$$

This cross section limit can be compared with predictions from SUSY calculations. The event generator of [16] has been used to simulate $\tilde{q}\tilde{q}$ and $\tilde{g}\tilde{g}$ production at the $\bar{p}p$ Collider. The final state jets have been submitted to the same very restrictive topological cuts as the data. Cross sections of about 10 pb are predicted for $\tilde{q}$ or $\tilde{g}$ masses in the range 40 to 60 GeV, whereas lower observable cross sections are expected for smaller or larger masses. The sensitivity to lower masses is suppressed due to the experimental selection criteria. The present analysis does not exclude events with such low cross sections and is therefore not in contradiction with the predictions of this specific model.

9. CONCLUSIONS

Preliminary results on jet physics from the data collected by the UA2 detector during the 1984 $\bar{p}p$ Collider run have been presented. The inclusive jet cross-sections showed the expected increase when comparing the $\sqrt{s}$= 630 GeV data to the $\sqrt{s}$ = 546 GeV data. A comparison of the inclusive jet cross section with a composite model places a lower limit on the compositeness scale of quarks to be $\Lambda_c > 370$ GeV (95% c.l.). The evidence for structure in the two-jet mass spectrum in the 1983 data sample was not confirmed by the 1984 data. The study of multi-jet events provided new tests of QCD. A status report on the search for exotic events with large $\not{p}_T$ was presented. There was no significant signal above background for either monojet or multi-jets and $\not{p}_T$.

REFERENCES

1. UA2 Collaboration, M. Banner et al., Phys. Lett. 118B (1982) 203.
UA2 Collaboration, P. Bagnaia et al., Z. Phys. C20 (1983) 117.
UA2 Collaboration, P. Bagnaia et al., Phys. Lett. 138B (1984) 430.

2. Axial Field Spectrometer Collaboration, T. Åkesson et al., Phys. Lett. 118B (1982) 185 and 193.

3. UA1 Collaboration, G. Arnison et al., Phys. Lett. 123B (1983) 115.

4. COR Collaboration, A.L.S. Angelis et al., Phys. Lett. 126B (1983) 132.

5. B. Mansouliè, The UA2 apparatus at the CERN $\bar{p}p$ Collider, proceedings 3rd Moriond workshop on $\bar{p}p$ physics, editions Frontières, 1983, p. 609;
M. Dialinas et al., The vertex detector of the UA2 experiment, LAL-RT/83-14, ORSAY, 1983;
C. Conta et al., Nucl. Instr. and Methods 224 (1984) 65;
K. Borer et al., Nucl. Instr. and Methods 227 (1984) 29.
A. Beer et al., Nucl. Instr. and Methods 224 (1984) 360.

6. M. Bozzo et al., Phys. Lett. 147B (1984), 392

7. T. Akesson et al., Phys. Lett. 118B (1982), 185,193
T. Akesson et al., Phys. Lett. 123B (1983), 133.

8. J.D. Bjorken, Phys. Rev. D8 (1973), 4098.

9. E. Eichten et al., Phys. Rev. Lett. 50 (1983), 811

10. B. L. Combridge, J. Kripfganz and J. Ranft, Phys. Lett. 70B (1977) 234 ;
see also : R. Cutler and D. Sivers, Phys. Rev. D17 (1978) 196.

E. Eichten et al., Rev. Mod. Phys. 56 (1984), 579.

11. F. Berends et al., Phys. Lett. 103b(1981) 124.
Z. Kunszt and E. Pietarinen, Phys. Lett. 132B (1983) 453.

12. G. Arnison et al., UA1 Collaboration, Phys. Lett. 139B, 115 (1984).

13. "The UA5 Streamer Chamber Experiment at the SPS $\bar{p}p$ Collider", The UA5 Collaboration, Phys. Scr. 23, 642 (1981).

14. ISAJET programme, written by F.Paige and S. Protopopescu, BNL report 31987 (1981).

15. P. Bagnaia et al., UA2 Collaboration, Z. Phys. C24, 1 (1984).

16. G. Kane and J.P. Léveillé, Phys. Lett. 112B, 227 (1982); P. Harrison and C.H. Llewellyn-Smith, Nucl. Phys. B213, 223 (1982); E B223, 542 (1983).

17. J. Ellis and H. Kowalski, Phys. Lett. 142B, 441 (1984); J. Ellis and H. Kowalski, Nucl. Phys. B246 189 (1984). J. Ellis and H. Kowalski, CERN-TH. 4072/84

18. B. Mansoulié, these proceedings.

FIGURE CAPTIONS

1. a) Comparison between the ratio of the inclusive jet cross-section at $\sqrt{s}$ = 546 GeV and at $\sqrt{s}$ = 630 GeV and the QCD calculations of ref. 10.
   b) Comparison between the ratio of the two-jet production cross-section at $\sqrt{s}$ = 546 GeV and at $\sqrt{s}$ = 630 GeV and the QCD calculation of ref. 10.

2. Invariant jet cross-section p_T^4 E $d\sigma/dp^3$ as a function of x_T both for ISR and UA2 data.

3. Comparison between the inclusive jet production cross-section presented in Fig. 1 and the expectations of the model of ref. 9 predicting quark and lepton compositeness (see text).

4. Two-jet invariant mass distribution
   (a) for 1983 data.
   (b) for 1984 data.

5. Acoplanarity distribution for three-jet events in an angular region where the two-jet contribution is negligible. The full line represents the QCD computation of ref. 11 for three-parton final states. The dashed line is the result of a calculation assuming a pure three-parton phase space.

6. Theoretical p_{Tout} distribution from ref. 11 using Λ = 200 MeV for two (dashed line) and three-parton (full line) final states compared with experimental data.

7. Scatter plot of event timing measured with the two veto counter arrays on both sides of UA2. Abscissa: timing of veto counter on incident proton side, ordinate:

timing of veto counter on incident anti-proton side. Only the events in the upper right hand side corner are genuine $\bar{p}p$ collisions.

8. Fig. 8: $\not{P}_T$-spectrum of final monojet sample (known $W \to e\nu$ events excluded). The smooth line is a Monte Carlo prediction by the ISAJET[14] programme for QCD 2-jet background.

9. Fig. 9: P_T spectrum of the monophoton candidates. For interpretation see text.

10. Fig. 10: $\not{P}_T$ spectrum of electromagnetic mono-clusters found through the $\not{p}_T$ analysis.

11. Energy deposition in FC for (a) events of this analysis, compared to (b) well-balanced QCD 2-jet events.

12. Angular distribution in transverse plane of the $\not{p}_T$ in FC with respect to the direction of the leading jet system in CC for a) the events of this analysis, b) well-balanced QCD 2-jet events.

a)

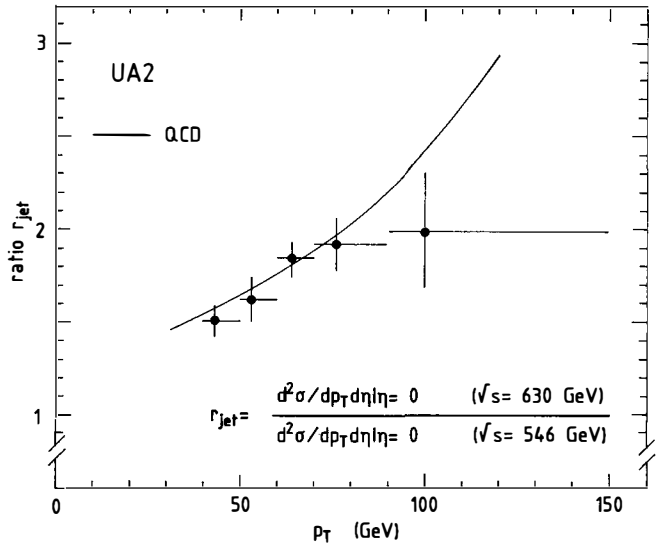
UA2
QCD
ratio r_{jet}
r_{jet}= $\frac{d^2\sigma/dp_T d\eta|\eta=0 \quad (\sqrt{s}= 630\ GeV)}{d^2\sigma/dp_T d\eta|\eta=0 \quad (\sqrt{s}= 546\ GeV)}$
p_T (GeV)

b)

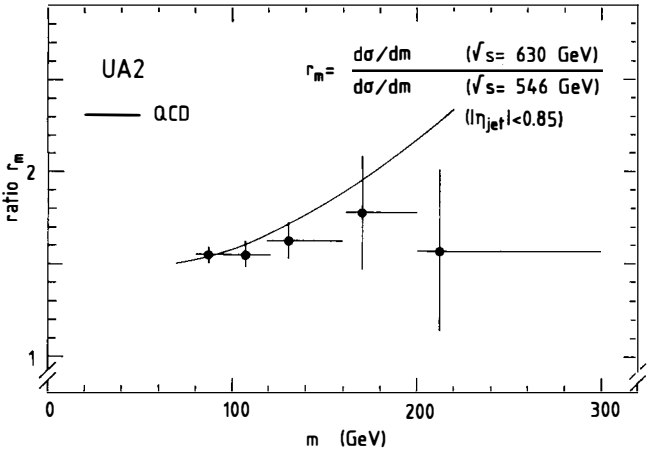
UA2
QCD
ratio r_m
r_m= $\frac{d\sigma/dm \quad (\sqrt{s}= 630\ GeV)}{d\sigma/dm \quad (\sqrt{s}= 546\ GeV)}$
$(|\eta_{jet}|<0.85)$
m (GeV)

Fig. 1

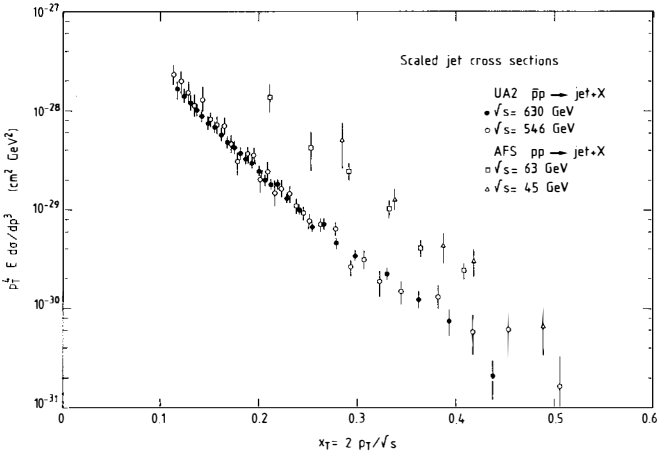
Scaled jet cross sections
UA2 p̄p → jet+X
• √s= 630 GeV
○ √s= 546 GeV
AFS pp → jet+X
□ √s= 63 GeV
△ √s= 45 GeV
$p_T^4 E\, d\sigma/dp^3$ (cm² GeV²)
$x_T = 2\, p_T/\sqrt{s}$

Fig. 2

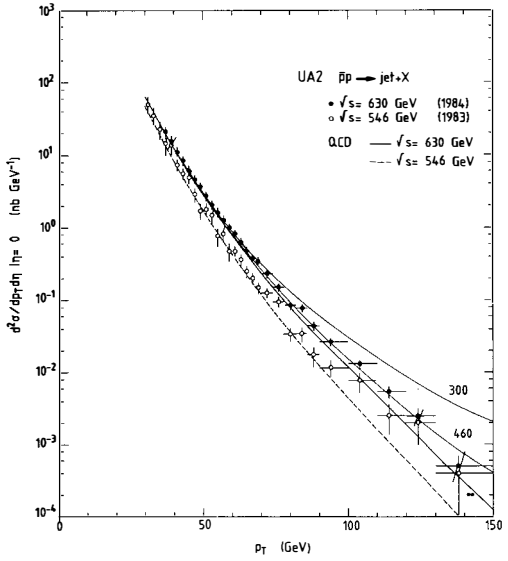
UA2 p̄p → jet+X
• √s= 630 GeV (1984)
○ √s= 546 GeV (1983)
QCD — √s= 630 GeV
--- √s= 546 GeV
300
460
$d^2\sigma/dp_T d\eta\,|\eta=0$ (nb GeV⁻¹)
p_T (GeV)

Fig. 3

a)

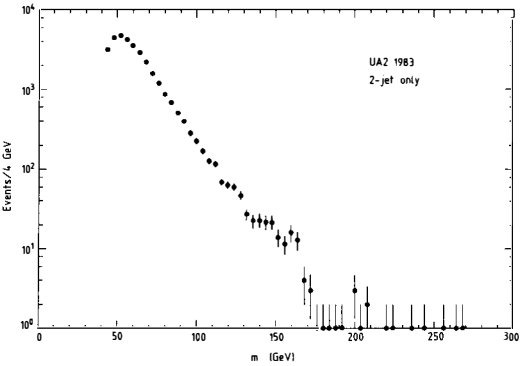
UA2 1983
2-jet only
Events/4 GeV
m (GeV)

b)

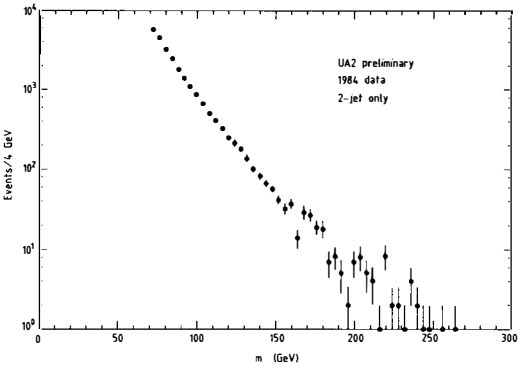
UA2 preliminary
1984 data
2-jet only
Events/4 GeV
m (GeV)

Fig. 4

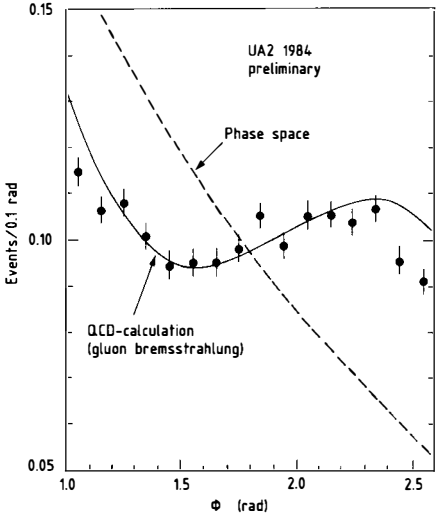
UA2 1984
preliminary
Phase space
QCD-calculation
(gluon bremsstrahlung)
Events/0.1 rad
Φ (rad)

Fig. 5

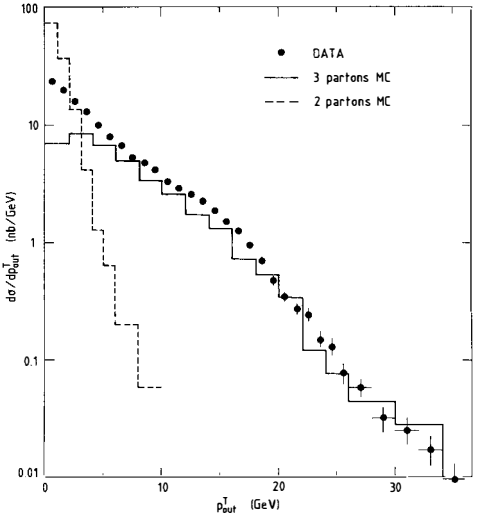
DATA
3 partons MC
2 partons MC
100
10
1
0.1
0.01
0
10
20
30
dσ/dp$_{out}^{T}$ (nb/GeV)
p$_{out}^{T}$ (GeV)

Fig. 6

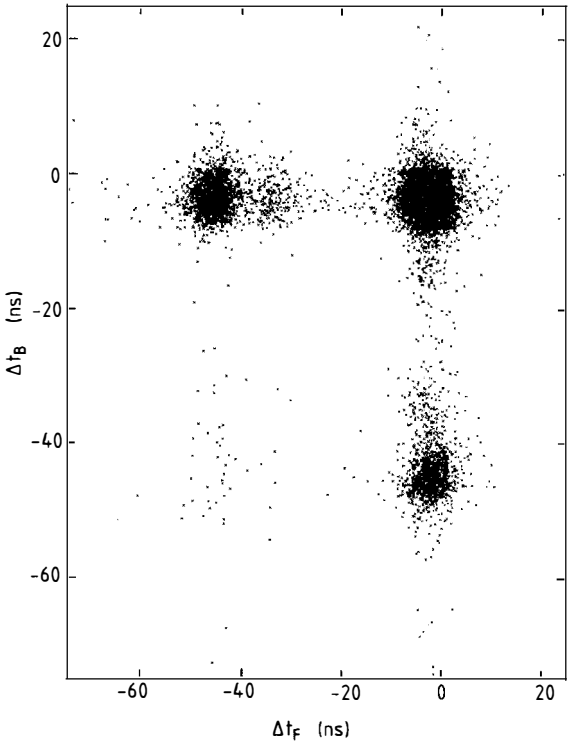
20
0
-20
-40
-60
Δt$_B$ (ns)
-60
-40
-20
0
20
Δt$_F$ (ns)

Fig. 7

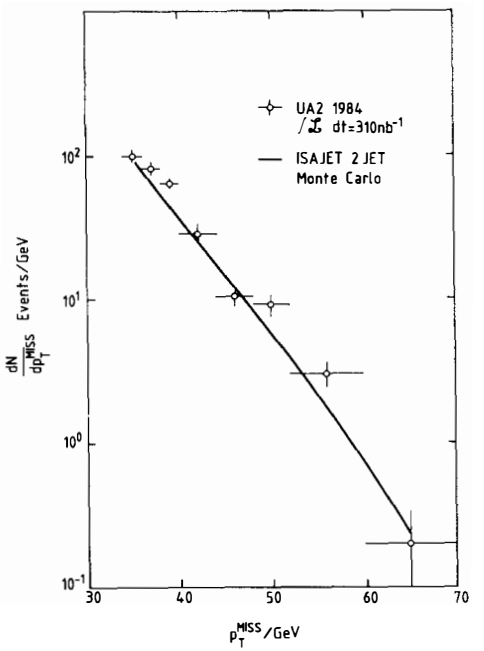

Fig. 8

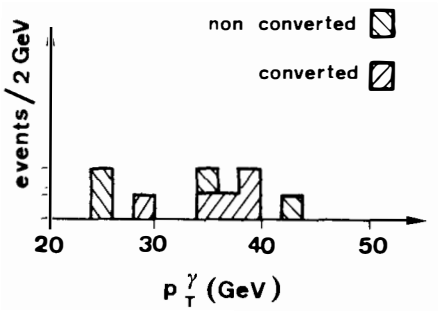

Fig. 9

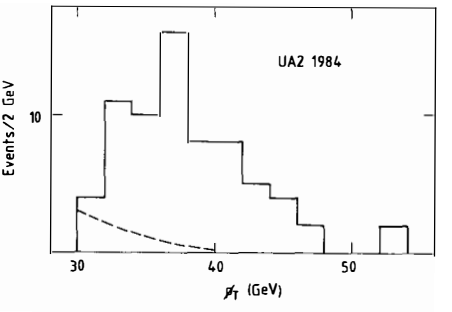

Fig. 10

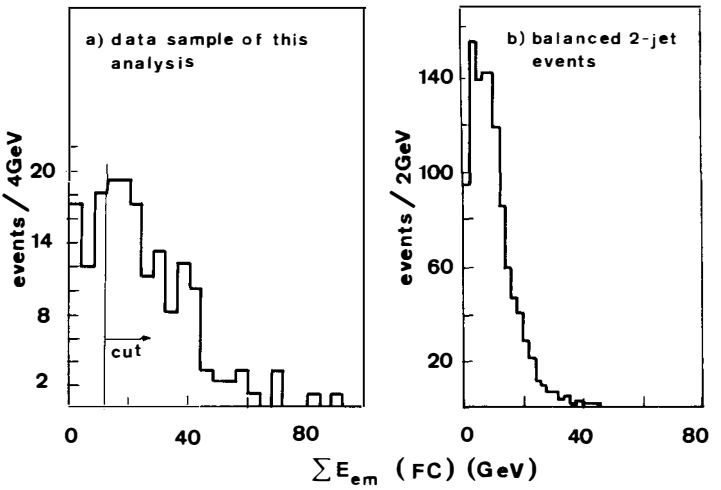
a) data sample of this analysis
b) balanced 2-jet events
events / 4GeV
events / 2GeV
cut
$\sum E_{em}$ (FC) (GeV)

Fig. 11

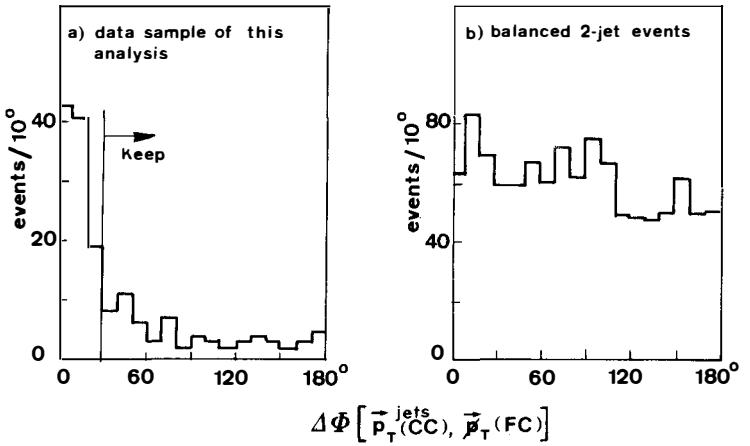
a) data sample of this analysis
b) balanced 2-jet events
events/10°
Keep
$\Delta\Phi\left[\vec{p}_T^{\,jets}(CC), \not{\vec{p}}_T(FC)\right]$

Fig. 12